SYNTHESIS AND CHARACTERIZATION OF NOVEL ORGANIC NONLINEAR OPTICAL CRYSTAL: L-PHENYLALANINIUM TARTRATE

Gershom Jebaraj, P.[1*], Sivashankar, V.[2]

[1]Department of Physics, St.Xavier's College (Autonomous), Affiliated to Manonmaniam Sundaranar University, Tirunelveli, India. [*]Corresponding author: *gershomjeba@gmail.com*

[2]Department of Physics, St.Xavier's College (Autonomous), Palayamkottai, Affiliated to Manonmaniam Sundaranar University, Tirunelveli, India.

Abstract. *L-Phenylalaninium Tartrate (LPT) organic NLO crystal was grown first of its time and subjected to various characterizations. Single crystal XRD studies were conducted. UV-visible spectral studies were carried out. Absorbance and transmittance spectra of LPT crystal were recorded. From the spectrum it is clear that the LPT crystal has a UV cut-off of approximately 265 nm. The band gap energy of the grown LPT crystal was calculated using the Tauc's plot and it is found to be 4.65 eV. PL spectrum of LPT crystal was recorded by exciting with UV light at 250 nm. The PL emission spectrum of LPT crystal contains the emission peaks at 468 and 543 nm in the visible region of the spectrum and the peak at 828 nm is due to the emission of IR radiation. FTIR spectral method was used to identify the presence of functional groups in the grown crystal. Microhardness study was performed by using a Microhardness analyser. Impedance analysis was carried out for LPT crystal by using an impedance analyser at different frequencies. From dielectric studies, it is observed that, the dielectric parameters like dielectric constant and loss factors decrease with increase in frequency and their values increase with increase in temperature. From the SHG measurement, it is observed that there is a green laser light emitted from the sample and the relative SHG efficiency of LPT sample is 1.71 times that of KDP sample. Z-scan technique was used to determine third-order NLO parameters of LPT crystal. LDT value was determined. The obtained value of LDT of LPT crystal is 2.675 GW/cm^2.*

Keywords. *single crystal; organic material; solution method; XRD; optical transmittance; micro-hardness; impedance; NLO; LDT;*

1. INTRODUCTION

Nonlinear Optical (NLO) materials play a major role in both academic research and technological applications. NLO crystals are the most suitable materials for frequency conversions, second harmonic generation, laser technology, optical data storage, optical switching and fibre optic communications [1]. Organic crystals possess higher non-linear efficiency compared to inorganic crystals. The organic crystals are effectively applied in active research due to its higher non-linear second order coefficients [2]. Amino acids play a promising role in NLO Applications as they possess proton acceptor amino group (NH_3^+) and a proton donor carboxyl group (COO^-) [3]. L-Phenylalanine is an amino acid, with surprisingly good SHG efficiency in it [4]. L-tartaric acid is a white crystalline organic material that occurs fruits, grapes, bananas, citrus and tamarinds and it forms many tartrate compounds [5].

2. EXPERIMENTAL METHOD

The organic single crystal of L-Phenylalaninium Tartrate was grown by dissolving high purity L-Phenylalanine and Maleic acid in 1: 1 molar ratio in a beaker containing 100 ml of double distilled water. The solution was stirred about 5 hours and heated in a constant temperature of about $50°C$. The prepared solution was filtered by Whatmann filter paper and left for slow evaporation at room temperature. Initially, seed crystals were obtained. By placing some of the good quality seed crystals in the saturated solution, big-sized crystals of LPT were grown. The schematic diagram of crystal growth process for growing LPT crystal is shown in figure 1 and the grown crystal is shown in figure 2. A good quality of LPT crystal of $25 \times 8 \times 7$ mm^3 size was obtained within one month. It is seen that the grown crystal is transparent and colourless.

3. RESULTS AND DISCUSSION

3.1 Single crystal XRD studies

The grown crystal of LPT is confirmed by single crystal XRD studies using ENRAF NONIUS CAD-4 diffractometer with MoK$_\alpha$ radiation (λ=0.71073 Å) to determine the crystal structure and lattice constants. From the analysis, the structure of the grown crystal is observed to be orthorhombic and the data are compared with the parent compound and are presented in Table 1.
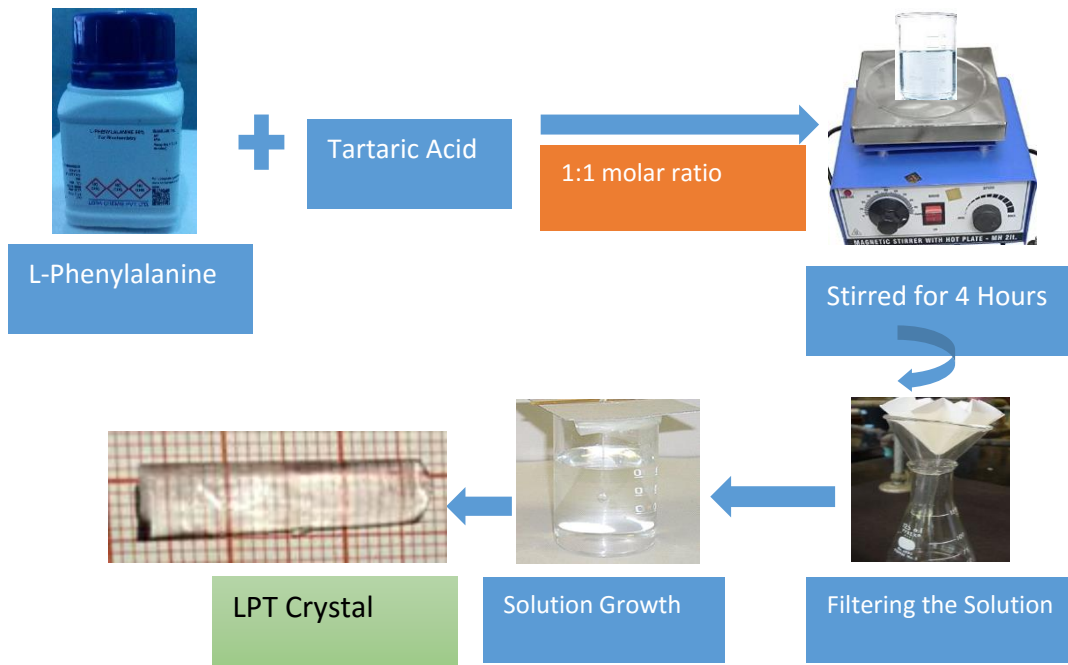
35

Fig: 1 Schematic diagram of Crystal growth process for growing LPT crystals

Fig.2 The grown bulk single crystal of LPT

Table 1 Unit cell parameters of LPT crystal

Parameters	LPT crystal
Crystal System	Orthorhombic
α	90º
β	90º
γ	90º
a (Å)	6.431 (2)
b (Å)	7.583 (4)
c (Å)	12.694(1)
Unit cell volume(Å^3)	619.04 (3)

3.2 UV-visible spectral studies

The optical properties of the grown crystal are studied by using UV-Vis analysis. The instrument used for recording UV spectrum is Perkin Elmer Lambda 35 spectrophotometer.

A graph of Absorbance vs Wavelength is drawn. It is shown in the figure 3. From the spectrum, it is clear that, the LPT crystal has a UV cut-off of approximately 265 nm. It reveals that, the grown crystal has good transmittance of nearly 80%, without the absorption peak in the entire visible region [6].

The Transmittance versus Wavelength graph was drawn and indicated by figure 4. From the graph, it is clear that the crystal has a wide transparency range, which enables it as a good candidate for NLO applications especially optoelectronic applications [7,8].

The band gap energy of the grown LPT crystal was calculated using the Tauc's plot and it is given in figure 5. The band gap is found to be 4.65 eV. This indicates that the LPT crystal is a higher band gap energy material.
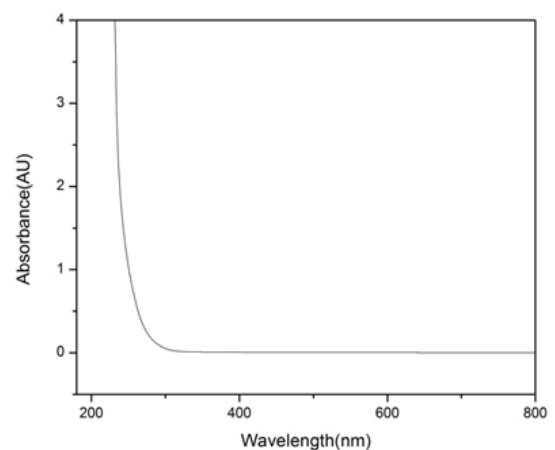

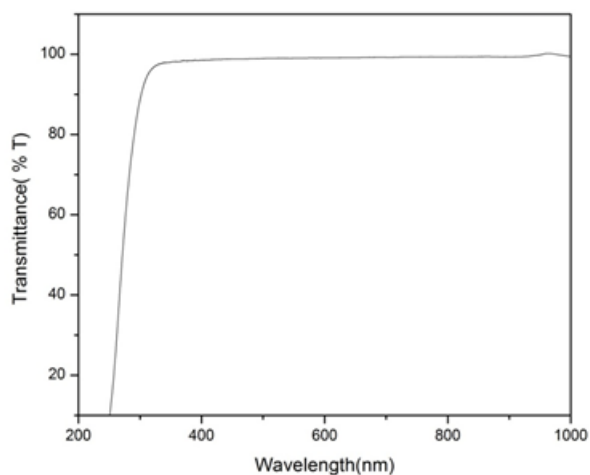**Fig. 3** UV-Vis absorbance spectrum of the grown LPT Crystal

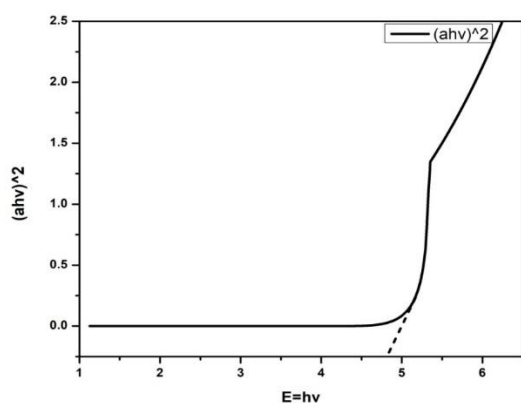**Fig. 4** UV-Vis transmittance graph of the grown LPT crystal

Fig. 5 Tauc's plot of the grown LPT crystal

3.3 Photoluminescence study

Photoluminescence (PL) is a phenomenon which generates optical radiation in UV, visible and IR spectral ranges when a sample is excited with UV light. PL is the emission of light radiation during the transition from its lowest vibrational energy level of the excited state back to its ground state. The loss of emission of photons is due to the vibrational relaxation, internal conversion and intersystem crossing. PL spectrum of LPT crystal was recorded at room temperature by exciting the crystal with UV light at 250 nm. The PL emission spectrum of LPT crystal is shown in the figure 6. From the result, it is observed that there are emission peaks at 468 and 543 nm in the visible region of the spectrum. The emission peak at 828 nm is due to the emission of IR radiation. The optical and electronic properties of the grown LPT crystal are studied by using photoluminescence analysis [9].
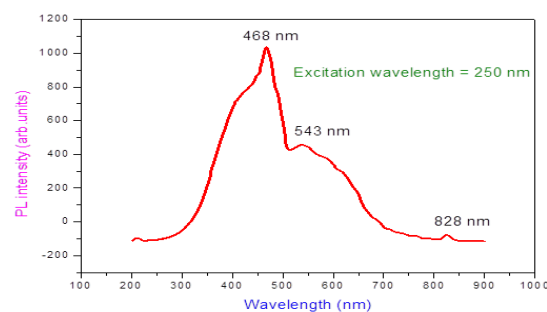

Fig. 6 Photoluminescence spectrum of the grown LPT crystal

3.4. FTIR spectroscopy

FTIR analysis was carried out to identify the presence of functional groups in the grown crystal. The characteristic absorption peaks was recorded in 400 – 4000 cm^{-1} using the Perkin Elmer FTIR Spectrometer and it is given in figure 7. The peak at 3168 cm^{-1} indicates the NH_3^+ stretching vibration and the peak at 3028 cm^{-1} corresponds to NH vibrational stretch [10]. The peak at 2048 cm^{-1} indicates the CH stretching. The peak at 1416 cm^{-1} indicates the presence of C=O stretch of COOH group [11]. The peak at 1347 cm^{-1} denotes the OH bend of COOH group [12]. The peak at 1041 cm^{-1} corresponds to C-H rocking vibration. The peak at 701 cm^{-1} indicates the in plane deformation of COO^- group.
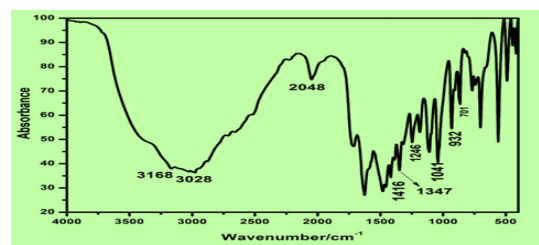

Fig. 7. FTIR spectrum of the grown LPT crystal

3.5 Microhardness studies

Measurement of hardness is a useful non-destructive testing method used to determine the applicability of the crystal in the device fabrication and it is one of the best methods to understand the mechanical properties of materials [13]. Crystals, free from cracks, with flat and smooth faces are chosen for Vickers Microhardness test [14]. For different loads of 25 g, 50 g, 75 g and 100 g, the indentations were applied at a constant indentation time with an interval of 25 s. Diagonal lengths of indentation (d) were noted in μm for different applied load (P) in g. The variation of diagonal length with applied load for LPT crystal is shown in figure 8. The Vickers hardness (H_V) number at different loads were calculated [15] using the following relation:

37

$$H_V = \frac{1.8544\,P}{d^2} \qquad (1)$$

Figure 9 shows the variation of Vickers hardness number (H_V) with the applied load (P). It is seen that the hardness number is increasing while increasing the applied load. Beyond 75 g, there is a slight decrease of hardness. It is because of formation of a crack on the surface of the sample.
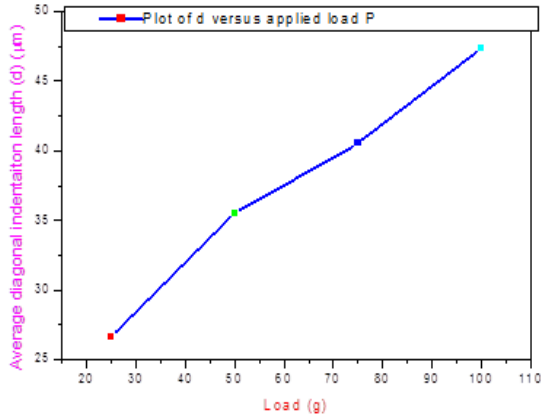

Fig.8 Variation of diagonal length with applied load for LPT crystal
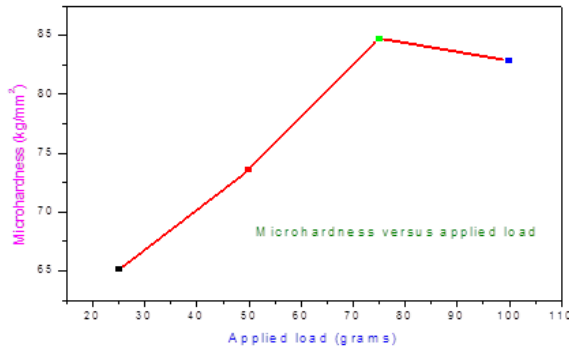

Fig.9 Variation of Microhardness with applied load for LPT crystal

Based on Meyer's analysis of hardness, relation connecting load P and indentation length d is

$$P = k_1 d^n$$

Where k_1 is the material constant, n is the Meyer's index or work hardening coefficient. Taking log on both sides of the above equation, it becomes

$$log P = log k_1 + n\, log d$$

A Plot of log P versus log d is shown in figure 10 and it yields a straight line graph. Its slope gives the value of work hardening coefficient (n) and it is found to be 3.102.
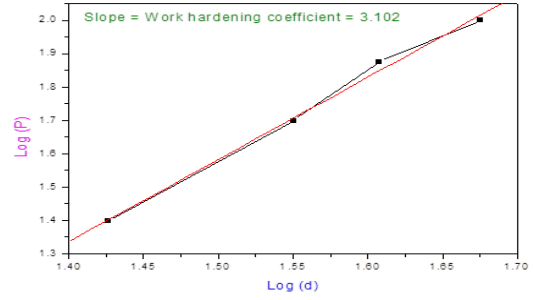

Fig. 10 Plot of log (d) versus log (P) for LPT crystal

According to Onitsch [16] and Hanneman [17], n value lies between 1 and 1.6 for hard materials and it is more than 1.6 for soft materials. Hence, LPT crystal belongs to soft material category. Kick's law states that since the material takes some time to revert to the elastic mode after every indentation, a correction term has to be applied to the d-value [18], and it is given by

$$P = k_2(d + x)^2$$
$$d^{n/2} = \left(\frac{k_2}{k_1}\right)^{1/2} d + \left(\frac{k_2}{k_1}\right) x$$

A graph is drawn between $d^{n/2}$ and d is shown in figure 11. This graph yields a straight line tendency with the slope of $(k_2/k_1)^{1/2}$ and with an intercept of $(k_2/k_1)\,x$. The obtained values of k_1, k_2 and x are tabulated in Table 2.
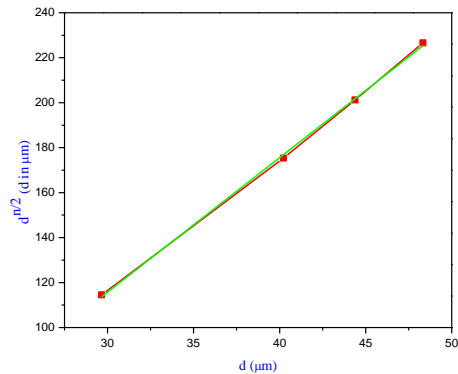
Fig. 11 Plot of $d^{n/2}$ versus d

Table 2 Values of the constants such as n, k_1, k_2 and x

Parameter	Value
n	3.1020
K_1 (kg/mm)	0.00251
K_2 (kg/mm)	0.05630
x	-7.4920

3.6. Impedance analysis

Impedance is defined as the frequency domain ratio of the voltage to the current and it is the opposition of the flow of alternating current (AC) in a complex system [19]. Impedance analyses were carried out for the grown crystal to find out the

impedance, bulk resistance, capacitance, DC conductivity and relaxation time [20]. This technique analyzes the ac response of a system to a sinusoidal perturbation and subsequent calculation of the impedance as a function of frequency of the perturbation [21]. The frequency dependent electrical properties of a material are often represented in terms of complex impedance $Z^* = Z' + jZ''$ where Z' is the real part of impedance and Z'' is the imaginary part of impedance [22]. Figure 12 gives the variation of real part of impedance with frequency at room temperature for LPT crystal. From the results, it is observed that the real part of impedance decreases with rise in frequency [23]. The high real part of impedance at low frequency indicates low ion mobility in the grown sample and it may result in improving NLO properties of the sample [24]. Figure 13 presents the variation of imaginary part of impedance (Z'') with frequency at room temperature for the grown crystal [25]. The Nyquist plot for LPT crystal is drawn between Z' versus Z'' and it is shown in the figure 14.
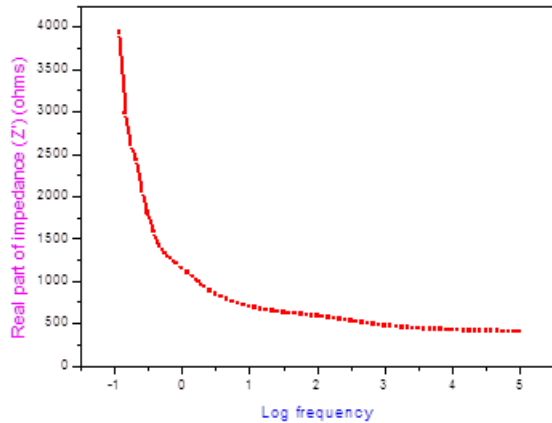

Fig.12 Variation of real part of impedance with frequency at room temperature for LPT crystal
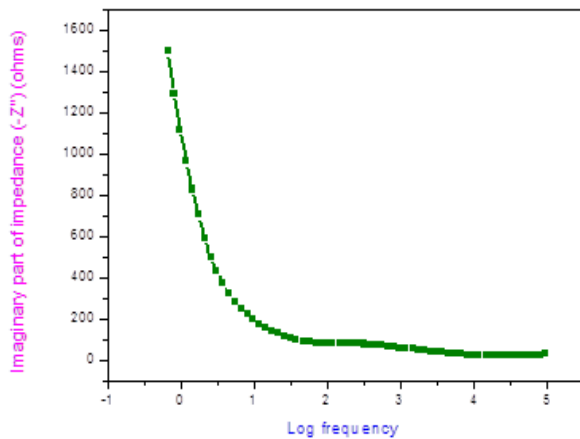

Fig.13 Variation of imaginary part of impedance with frequency at room temperature for LPT crystal
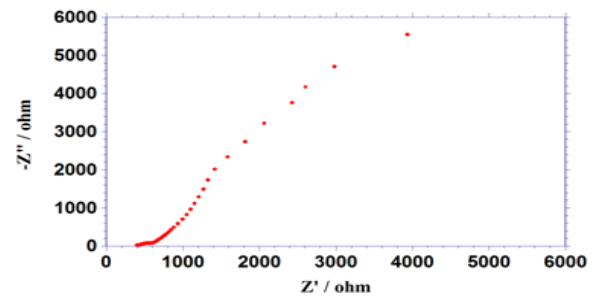

Fig.14 Nyquist plot for LPT crystal

3.7. Dielectric measurement

Dielectric studies were carried out to investigate the response of the crystal to an applied electric field and to determine various electrical parameters such as dielectric constant (ε_r), dielectric loss (tan δ) and conductivity at different temperatures [26]. Occurrence of a dielectric between the plates of a condenser increases the capacitance. Essentially, dielectric constant is the measure of how easily a material is polarized in an external electric field [27]. Dielectric parameters depends on the frequency applied and temperature. The variations of dielectric parameters of the samples with temperatures and frequencies are presented in the figures 15 and 16. From the graphs, it is observed that dielectric parameters like dielectric constant and loss factor decrease with increase in frequency and their values increase with increase in temperature. The high values of ε_r at low frequencies may be due to presence of space charge polarization. Its low value at high frequencies is because of the loss of four polarizations viz. space charge, orientational, ionic and electronic polarization. It is to be noted here that, the space charge polarization is dominant whereas electronic and ionic polarizations are not very much active in low frequency range and the low value of dielectric constant at higher frequencies will be due to the reason of the slagging of dipoles with respect to the quick changes in the applied field. It is a suitable parameter for the enhancement of SHG coefficient and extending the samples application towards photonic, electro-optic and NLO devices [28]. Increase of dielectric constant with temperatures may be due to the thermal excitation of atoms about their lattice point and blocking of charge carriers at the electrodes [29]. It is observed that at lower frequencies and higher temperatures, the dielectric constant and dielectric loss of the sample is larger [30]. High dielectric constant values of the sample leads to power dissipation. A material having low dielectric constant will have less number of dipoles per unit volume and as a result, it may have

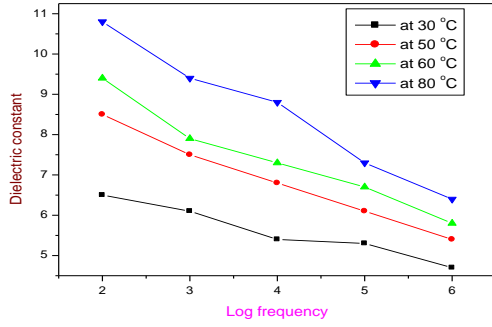minimum loss compared to the material having high dielectric constant.

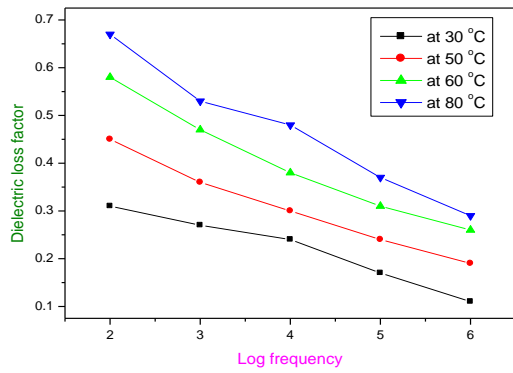**Fig.15** Variation of dielectric constant with frequency at different temperatures for LPT crystal

Fig.16 Variation of dielectric loss with frequency at different temperatures for LPT crystal

3.8. Second-order NLO studies

Second harmonic generation (SHG) is an optical process that results in the conversion of an input optical wave into an output optical wave with a frequency twice that of the input wave. This frequency doubling process is particularly used to make green laser light with a wavelength of 532 nm from an Nd: YAG laser operates at 1064 nm. Kurtz and Perry powder method is used for analyzing the SHG efficiency of the sample [31]. The laser is focused on a powdered sample, and the light emitted is collected, filtered and detected using a photomultiplier tube [32]. The primary laser beam with a wavelength of 1064 nm, and a pulse width of 6 ns, and a pulse rate of 10 Hz are made to fall on the powdered LPT crystal sample. In this experiment, the reference sample used is KDP [33]. The obtained data from the SHG experiment for the LPT sample are given in table 3. From the SHG data, it is observed that there is a green laser light emitted from the sample, and hence LPT sample shows the second-order NLO effect. The result indicates that the relative SHG efficiency of LPT sample is 1.71 times that of KDP sample [34].

Table 3 SHG data for LPT crystalline material

Sl. No.	Sample Code / Name of the sample	Output Energy (milli joule)	Input Energy (joule)
1	KDP (Reference)	8.90	0.70
2	LPT sample	15.22	0.70

3.9. Third-order NLO studies-Z-scan technique

There are two modes of measurement in the Z-scan technique, viz. open aperture and closed aperture modes. A He–Ne laser (λ = 632.8 nm) is utilized as the light source in this measurement. The light intensities are determined as a function of sample location in the Z-direction relative to the focal plane using closed or open aperture techniques to resolve the nonlinear refraction and absorption coefficients [35]. The relation between transmission difference between peak and valley (ΔT_{p-v}) from closed aperture Z-scan curve and the phase shift ($\Delta\phi$) is given by

$$\Delta T_{p-v} = 0.406(1 - S)^{0.25}|\Delta\phi|$$

Here S is the linear transmittance aperture. Using the above relation, the phase shift ($\Delta\phi$) is determined, and using this value, the third-order nonlinear refractive index (n_2) is calculated using the following relation

$$n_2 = \Delta\phi \ / \ KI_0 L_{eff}$$

where I_o is the intensity of the laser beam at the focus, L_{eff} is the effective thickness of the sample, and K is the wave vector [36]. In the closed aperture Z-scan curve, the nonlinear absorption coefficient (β) can be determined using the following relation

$$\beta = 2\sqrt{2}\Delta T \ / \ I_0 L_{eff}$$

Where ΔT is the peak value of the Z-scan curve for an open aperture." The value of β will be negative in the case of saturable absorption and positive in the case of two-photon absorption"[37]. The following relations can be used to derive the real and imaginary components of the third-order nonlinear susceptibility ($\chi^{(3)}$).

Real part of $\chi^{(3)} = (10^{-4}\varepsilon_0 c^2 n_0^2 n_2^2) \ / \ \pi$

Imaginary part of $\chi^{(3)} = (10^{-2}\varepsilon_0 c^2 n_0^2 \lambda\beta) \ / \ 4\pi^2$

Where ε_o is the permittivity of free space or vacuum, n_o is the linear refractive index of the sample, λ is the wavelength of light and c is the velocity of the light [38-39].

The open aperture and closed aperture Z-scan curves for LPT crystal are shown in figures 17 and 18 respectively. Since the closed aperture curve shows a peak followed by a valley, LPT crystal has the negative value of the nonlinear refractive index, and it is due to non self-defocusing nature. The important values in connection with the Z-scan analysis are provided in table 4. From the obtained data, the nonlinear third-order optical susceptibility

of LPT crystal is observed to be high and hence this crystal could be useful in NLO applications.
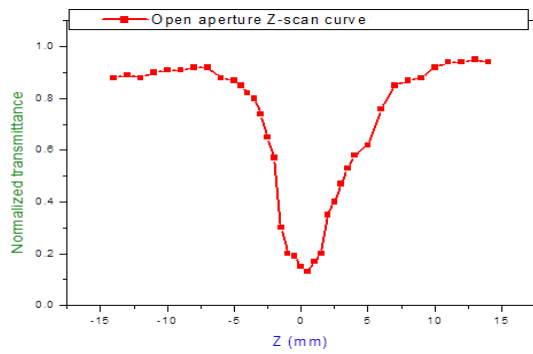

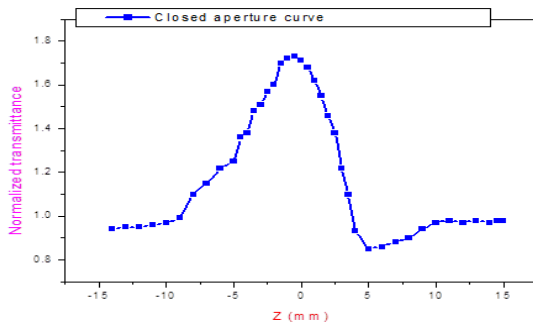**Fig. 17** Open aperture Z-scan curve of LPT crystal

Fig. 18 Closed aperture Z-scan curve of LPT crystal

Table 4 Z-scan data for LPT crystal

Important parameters	Values
Laser wavelength (λ)	632.8 nm
Lens focal length	30 mm
Aperture radius (r_a)	4.1 mm
Spot size in front aperture (ω_a)	4.5 mm
Incident intensity	2 MW/cm^2
Sample thickness	0.77 mm
Nonlinear absorption coefficient (β)	3.024×10^{-5} m/W
Nonlinear refractive index (n_2)	- 6.247×10^{-9} m^2/W
Real part of third-order susceptibility	5.402 ×10^{-7}esu
Imaginary part of third-order susceptibility	7.551×10^{-8}esu
Third-order susceptibility, $\chi^{(3)}$	5.448×10^{-7}esu

3.10 Laser damage threshold measurement

An important related property of NLO crystals is the threshold for catastrophic laser induced damage. Laser induced damage in optical materials is a phenomenon involving interaction of high power laser radiation with matter and various physical, chemical, mechanical, optical and other aspects of materials that come into play. It is evident that the harmonic conversion efficiency is proportional to the power density of the fundamental beam. Hence, a convenient way to increase the efficiency is to focus the beam into the crystal. But, this often leads to breakdown of the materials, catastrophically damaging the crystal. It is then useful to prescribe the maximum permissible power for a particular crystal, defined as damage threshold.

The minimum power level which causes damage to at least 50% of irradiated sites is defined as the single shot damage threshold. Laser damage threshold is a special parameter of a material. Before applying a crystal as an NLO component in various applications such as frequency doubling, optical parametric processes etc., one should calculate the LDT value of the particular crystal [40]. LDT measurement was conducted for the crystal at 1064 nm. The laser damage threshold depends on pulse duration, focal spot geometry, sample quality, previous history of the sample, experimental technique employed etc. The experimental set-up used for the measurement of laser damage of the samples is shown in figure 19. A Q-switched Nd: YAG laser (Continuum USA, Model: Surelite-III) of wavelength 1064 nm and pulse width of 10 ns was used. The energy of the laser pulse was controlled by an attenuator (combination of λ/2 plate and polarizer) and delivered to the test sample located near the focus of a plano-convex lens of focal length 30 cm. The presence of single pulse damage was found by checking the fall of transmitted intensity as determined by a fast PIN type Si photodiode and drawn in a digital storage oscilloscope (Tektronix:TDS 3054B). A pyro-electric energy meter was used for measuring the energy of the input laser pulse for which the crystal gets damaged. The LDT value was determined using the formula P = E/$\pi\tau r^2$ where E is the input energy in mJ, τ is the pulse width in ns and r is radius of the laser spot in mm [41, 42]. The calculated value of LDT of LPT crystal is 2.675 GW/cm^2. Since this value of high, LPT crystal could be used for laser applications [43].
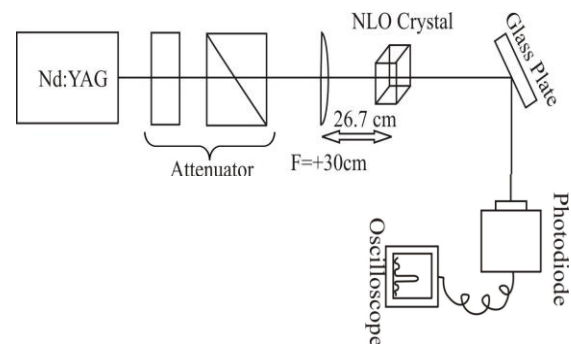

Fig. 19 Block diagram for the laser damage threshold measurement

4. CONCLUSIONS

In the present study, an organic NLO crystal viz. L-Phenylalaninium Tartrate (LPT) was grown first of its time and subjected to various characterizations. The grown crystal of LPT is subjected to single crystal XRD studies. From the analysis, the structure of the grown crystal is found to be orthorhombic. UV-visible spectral studies were carried out by using a spectrophotometer. Absorbance and transmittance spectra of LPT crystal were recorded. From the spectrum it is clear that the LPT crystal has a UV cut-off of approximately 265 nm, reveals that the grown crystal has good transmittance of nearly 80% without the absorption peak in the entire visible region. The band gap energy of the grown LPT crystal was calculated using the Tauc's plot and it is found to be 4.65 eV. PL spectrum of LPT crystal was recorded by exciting with UV light at 250 nm. The PL emission spectrum of LPT crystal contains the emission peaks at 468 and 543 nm in the visible region of the spectrum and the peak at 828 nm is due to the emission of IR radiation. FTIR spectral method was used to identify the presence of functional groups in the grown crystal. The functional groups identified are NH_3^+, NH, CH, C=O, CN, COO^- etc. Microhardness study was performed by using a Microhardness analyser and it is found that hardness increases with increase in applied load up to 75 g and then it decreases. Meyer's law was used to calculate the value of work hardening coefficient and it is found to be 3.102. Impedance analysis was carried out for LPT crystal by using an impedance analyser at different frequencies. From the results, it is observed that the real part of impedance decreases with rise in frequency and also imaginary part of impedance decreases with increase in frequency. The Nyquist plot for LPT crystal was also drawn between Z' versus Z". From dielectric studies, it is observed that, the dielectric parameters like dielectric constant and loss factors decrease with increase in frequency and their values increase with increase in temperature. The high values of ε_r at low frequencies may be due to the presence of space charge polarization and its low value at high frequencies may be due to the loss of four different type of polarizations such as space charge, orientational, ionic and electronic polarization. The low value of dielectric constant at higher frequencies will be due to the reason of the slagging of dipoles with respect to the quick changes in the applied field. From the SHG measurement, it is observed that there is a green laser light emitted from the sample and the relative SHG efficiency of LPT sample is 1.71 times that of KDP sample. Z-scan technique was used to determine third-order NLO parameters of LPT crystal by using a He–Ne laser ($\lambda = 632.8$ nm). From the obtained data, the nonlinear third-order optical susceptibility of LPT crystal is observed to be high and hence this crystal could be useful in NLO applications. The LDT value was determined. The obtained value of LDT of LPT crystal is 2.675 GW/cm^2. Hence the grown LPT crystal shall be used in Laser applications also.

5. REFERENCES

[1] Siva Shankar, R. Siddheswaran, R. Sankar, R. Jayavel, P. Murugakoothan, Mater.lett, Growth and characterization of new semiorganic nonlinear optical single crystal L- Phenylalanine L – Phenylalaninium perchlorate (LPPAPC), 63, 363-365. 2009, https://doi.org/10.1016/j.matlet.2008.10.049

[2] Jerin susan John, T. Arumanayagam, P. Murugakoothan, D. Sajan, Nithin Roy, Synthesis, growth and characterization of guanidinium hippurate monohydrate single crystals: A new third order nonlinear optical material, Opt.Mater., 110, 110493. 2020 http://www.elsevier.com/locate/optmat

[3] Siddheswaran, V. Siva Shankar, R. Jayavel, P. Murugakoothan, Int.J.Mater.Sci, 4(3), 205 – 213. 2009. http://www.ripublication.com/ijoms.htm

[4] Manimaran, P. Paramasivam, S. Bhuvaneshwari, R.S.Abina Shiny, B. Ravindran, M. Mariappan, Growth and characterization of L threonine doped potassium sulphate; A new Nlo semi organic crystal, Res.Rev. Int. J. Multidisci., 4(3), 2455-3085. 2019 www.rrjournals.com

[5] Thilagavathi, R. Arun kumar, A. Kumaresh, N. Ravi kumar, Growth and characterization of L- Threonine dopepd thiourea single crystals: an optical material, Mater.Res.Innovat., 20 (4), 254 – 258. 2016. https://doi.org/10.1080/14328917.2015.1105569

[6] Manju Kumari, N Vijayan, Debabrata Nayak, Mahesh Kumar, Govind Gupta and R P Pant, Assessment of optical, mechanical and nonlinear properties of potassium acid phthalate single crystal: a potential candidate for optoelectronic applications, Mater. Res. Express 7, 015705, 2020, 11 pages, https://iopscience.iop.org/article/10.1088/2053-1591/ab619e

[7] Senthil kumar, C. Ramachandraraja, Growth, Structural, Spectral and Optical Studies on Pure and L-Alanine Mixed Bisthiourea Cadmium Bromide (LABTCB) Crystals , J. of Minerals and Materials Characterization and Eng, Sci.Res, 11(6), 631-639. 2012 DOI: 10.4236/jmmce.2012.116046

[8] Suba, P. Selvarajan, J. Jebaraj Devadasan, Rubidium chloride doped magnesium oxide nanomaterial by using green synthesis and its characterization, Chemical Physics Letters, 793, 2022, 139463. https://doi.org/10.1016/j.cplett.2022.139463

[9] Indumathi, K. Deepa, S. Senthil, Growth and characterization of L threonine Lithium chloride: A new semiorganic non linear optical single crystal, IJDER, 5(1), 560-564. 2017. IJEDR1701084, www.ijedr.org

[10] Kalaiarasi, M. Senthil kumar, S. Shanmugan, T. Jarin, V. Chithambaram, Kishor kumar Sadasivuni and M.Nagarajan, Synthesis and characterization of L threonine ammonium bromide: grown on single crystal with experimental studies on NLO, Bull.Mater.Sci,

44:175. 2021. https://doi.org/10.1007/s12034-021-02421-6

[11] Hanumantharao Redrothu, S. Kalainathan, G. Bhagavannarayana, Crystal growth and characterization of novel non linear optical crystal: L – threonine formate, AIP Conf.Proc, 1447, 1311-1312, 2012. https://doi.org/10.1063/1.4710495

[12] Smallman and A.H.W. Ngan, Characterization and analysis, Modern physics metallurgy (eighth edition), Butterworth Heinemann, 159-250, 2014. https://doi.org/10.1016/B978-0-08-098204-5.00005-5

[13] Gale, T.C. Totemeier, Mechanical testing, Smithells Metals Reference Book (Eighth Edition), Butterworth-Heinemann, 2004, 21-1-21-23, https://doi.org/10.1016/B978-075067509-3/50024-5.

[14] Hanumantharao and S. kalainathan, Microhardness studies on nonlinear optical L-alanine single crystals, Bulletin of Materials Science, 36(3), 2013, DOI:10.1007/s12034-013-0500-1

[15] Jyotsna R pandey, Shaila wagle, Vicker's Microhardness Studies and 1H-NMR Spectral Analysis of an Organic NLO Material , IJARIIE, 3(5), 2017, 1433-1440,

[16] Onitsch, The Present Status of Testing the Hardness of Materials, Mikroskopie, 95(15), 1956. 12-14.

[17] Hanneman and J. H. Westbrook, Effects of adsorption on the indentation deformation of non-metallic solids, Series 8, 18 (151), 1968, 73-88 , https://doi.org/10.1080/14786436808227310

[18] Jaroslava Svobodova , Irena Lysonkova and Miroslav Krejci, Microhardness and Nano-hardness Measurement of Composite Coatings Applied to Aluminium Substrate, 2019, 19(4), Manufacturing Technology, 700-705, 10.21062/ujep/358.2019/a/1213-2489/MT/19/4/700 , https://journalmt.com/pdfs/mft/2019/04/27.pdf

[19] Mohammad Aljarrah and Fathy Salman, A simple analysis of impedance spectroscopy : Review, Journal of the institutions of Engineers (India) ; series D, 102(18), 1-6, 2021, DOI:10.1007/s40033-021-00252-7

[20] Chen, Chen Cheih yen, C.S.Shern, T. Fukami, Impedance spectroscopy and dielectric analysis in KH2PO4 single crystal, Solid State Ionics, 177(33-34), 2857-2864, 2006, DOI:10.1016/j.ssi.2006.05.053

[21] Dong Ming, J.M. Reau, J. Ravez, Joo Gitae and P. Hagenmuller, Impedance-Spectroscopy Analysis of a LiTaO3-Type Single Crystal, Journal of Solid State Chemistry,116(1), 185-192, 1995.https://doi.org/10.1006/jssc.1995.1200

[22] Hongwei Huang, Xiqi Feng, and Zhenyong Man, Impedance spectroscopy analysis of La-doped PbWO4PbWO4 single crystals, Journal of Applied Physics, 93, 421, 2003. https://doi.org/10.1063/1.1519956

[23] Daria Vladikova, J.A Kilner, Stephen J Skinner and Gergava Raikova, Differential impedance analysis of single crystal and polycrystalline yttria stabilized zirconia, Electrochimica Acta 51(8):1611-1621, 2006, DOI:10.1016/j.electacta.2005.02.110

[24] Rathna, V. S. John, T. Chithambarathanu and P. Selvarajan, Growth, Spectral, NLO and Impedance Studies of Potassium Ammonium Sulphate crystals grown by Aqueous Solution technique, International Journal of Applied and Advanced Scientific Research (IJAASR), 2(2), 304-311, 2017, https://core.ac.uk/download/pdf/144709301.pdf

[25] Deepthi, A. Sukhdev, P.M. Kumar, Growth and impedance analysis of pure TGAc and dye doped TGAc crystals-enhanced dielectric permittivity for energy-storage devices, SN Appl. Sci. 2, 1493, (2020). https://doi.org/10.1007/s42452-020-03295-9.

[26] Suresh Sagadevan and Priya Murugasen, Growth, Microhardness, Electrical and Dielectric Studies on L-Alanine Hydrogen Chloride NLO Single Crystal, International Journal of Materials Science and Engineering,3(2), 159-166, 2015, doi: 10.17706/ijmse.2015.3.2.159-166.

[27] Koteeswari, P. Mani, Sagedevan suresh, Optical and Dielectric Studies on L-Valinium Picrate Single Crystal, Journal of Crystallization Process and Technology, 02(03) , 2012, DOI:10.4236/jcpt.2012.23015.

[28] Ashim Kumar Bain, Prem Chand, Dielectric Properties of Materials, Ferroelectrics: Principles and Applications, 2017, 1-18 , DOI:10.1002/9783527805310.ch1

[29] Stuart O. Nelson & Andrzej W. Kraszewski, Dielectric Properties of Materials and Measurement Techniques, Drying Technology, 8:5, 1123-1142, 1990, DOI: 10.1080/07373939008959939.

[30] Muhammad Taha Jilani, Muhammad Zaka ur Rehman, Abid Muhammad Khan, Muhammad Talha Khan, Syed Muzamil Ali, A Brief Review of Measuring Techniques for Characterization of Dielectric Materials International Journal of Information Technology and Electrical Engineering, 1(1), 2012, 5 pages, http://www.iteejournal.org/archive/vol1no1/v1n1_1.pdf

[31] Kurtz and T. Perry, A powder technique for the evaluation of nonlinear optical materials. J.Appl.Phys. 39, 3798 (1968).

[32] Xu, R.W. Boyd, G.L. Fischer, Nonlinear Optical Materials, Reference Module in Materials Science and Materials Engineering, Elsevier, 2016, https://doi.org/10.1016/B978-0-12-803581-8.02404-8

[33] Dadap and T.F. Heinz, Spectroscopy , Second-Harmonic Spectroscopy, Encyclopedia of Modern Optics, Elsevier, 2005, 134-147, https://doi.org/10.1016/B0-12-369395-0/00907-6.

[34] Aravind P. Anthur, Haizhong Zhang, Ramon Paniagua-Dominguez, Dmitry A. Kalashnikov, Son Tung Ha, Tobias W. W. MaB, Arseniy I. Kuznetsov, and Leonid Krivitsky, Continuous Wave Second Harmonic Generation Enabled by Quasi-Bound-States in the Continuum on Gallium Phosphide Metasurfaces, Nano Letters, 20 (12), 8745-8751, 2020, DOI: 10.1021/acs.nanolett.0c03601

[35] Mezher, A. Nady, R. Penny, W. Y. Chong, and R. Zakaria, Z-scan studies of the nonlinear optical properties of gold nanoparticles prepared by electron beam

deposition, Appl. Opt. 54, 9703-9708, (2015) https://doi.org/10.1364/AO.54.009703

[36] Marziyeh Parishani, Marzieh Nadafan, and Rasoul Malekfar, Z-scan investigation to evaluate the third-order nonlinear optical properties of cauliflower-like VS_2 structures, journal of the Optical society of America B, 38, 1586-1592, 2021, https://doi.org/10.1364/JOSAB.418182

[37] Marta Gordel, Radoslaw Kolkowski, Joanna Olesiak-Banska, Katarzyna Matczyszyn, Malcolm Buckle and Marek Samoc, Z-scan studies of nonlinear optical properties of colloidal gold nanorods and nanoshells, Journal of Nanophotonics, 9(1), 093797, 2014. https://doi.org/10.1117/1.JNP.9.093797

[38] Ashok kumar and Rajamani. Growth, Crystalline Perfection and Z-scan Studies of Nonlinear Optical alpha-Lithium Iodate Single Crystal, Journal of Pure Applied and Industrial optics, 1(1), 61-67, 2010.

[39] Rajan, Rejeena V. George, Merin , D.R. Leenaraj, Reena Ittyachan, D Sajan, G. Vinitha, Growth, Z-scan and density functional theoretical study for investigating the nonlinear optical properties of guanidinium L-glutamate for optical limiting applications, Journal of Molecular Structure, 1222, article id. 128937, 2020, DOI:10.1016/j.molstruc.2020.128937

[40] Bastian Schwarz, Gunnar Ritt, Michael Koerber, Bernd Eberle, Laser-induced damage threshold of camera sensors and micro-optoelectromechanical systems, Optical Engineering, 56(3), 034108, 2017. https://doi.org/10.1117/1.OE.56.3.034108

[41] Albertas Zukauskas, Gintare Bataviciute, Mindaugas Sciuka, Tomas Jukna, Andrius Melninkaitis, and Mangirdas Malinauskas, Characterization of photopolymers used in laser 3D micro/nanolithography by means of laser-induced damage threshold (LIDT), Opt. Mater. Express 4, 1601-1616, 2014.

[42] Kannan, D Jayaraman, S Aravindhan, A study on the growth optical, thermal, dielectric, laser damage threshold and mechanical properties of amaranth dye doped thiourea single crystals, International journal of current research, 7(3), 2015, 13878-13887.

[43] Jauhar and P Murugakoothan, Synthesis, growth, optical and laser damage threshold studies of diphenylacetic acid single crystals, Conference: National Laser Symposium 24 , At: RRCAT, Indore, 2015.